Supplement

Materials and Methods

Human subjects. Informed consents were obtained from all subjects (or their guardian) for these studies in accordance with Helsinki principles for enrollment in research protocols that were approved by the Institutional Review Boards of NIAID, Yale, or Baylor. Blood from anonymous healthy donors was obtained from the NIH Clinical Center or purchased from the New York Blood Center under approved protocols.

Whole-exome and Sanger sequencing. Genomic DNA was extracted from peripheral blood cells and used for SureSelect Human All Exon 50 Mb kit (Agilent) selection followed by next-generation sequencing on an Illumina HiSeq Sequencing System with 50-100x coverage. The DNA reads were mapped to the hg19 human genome reference using Burrows-Wheeler Aligner, and variant calling was performed using the Genome Analysis Toolkit (the Broad Institute) and SeattleSeq Annotation tool. After filtering and prioritizing variants, heterozygous *PIK3CD* variants were investigated further since the clinical characteristics of the patients were consistent with APDS. For confirmation of mutations, *PIK3CD* genomic DNA was PCR amplified and subjected to Sanger sequencing after PCR purification. Whole-exome data will be deposited in dbGap.

Cell culture and transfection. Human T cells were isolated from patient or healthy donor peripheral blood by EasySep Direct Human T Cell Isolation Kit (STEMCELL Technologies) and resuspended at a density of 1×10^6 cells per ml in complete RPMI-1640 medium (Lonza) containing 10% fetal bovine serum (FBS), 2 mM glutamine, and penicillin and streptomycin (100 U/ml each; Invitrogen). Transfection was performed with Amaxa Nucleofection kits (Lonza) for primary cells and with standard electroporation for human cells and evaluated 24 hours post-transfection. Inhibitor studies were performed by pre-treating activated T cell blasts with 100-200 nM idelalisib (also called CAL101 or GS1101; purchased from Cayman Chemicals) for 30-60 min before fixing cells and performing flow cytometry for the indicated phosphosites.

Flow cytometry. For standard surface staining, PBMCs (1×10^6 cells per sample), sorted cells, expanded T cell populations or cell lines were washed with PBS and incubated for 30 min at 4 °C (in the dark) in 100 µl 5% FBS in PBS with the appropriate fluorochrome-labeled monoclonal antibodies or their isotype-matched control antibodies. After two washes with PBS, 1×10^4 to 5×10^4 live cells were analyzed by flow cytometry. For Phosflow staining, unless otherwise indicated, cells were kept in complete RPMI-1640 medium while alive, then were fixed directly in complete RPMI-1640 medium with BD Lyse-Fix and then permeabilized with Perm Buffer III according to manufacturer's instructions (BD). The following validated antibodies were used for flow cytometry: anti-CD20 (2H7; BioLegend); anti-CD27 (M-T271), anti-CD10 (HI10A), anti-CD8 (RPA-T8); all from BD Biosciences); anti-CD3 (HIT3α (BioLegend) or UCHT1 (BD Biosciences), anti-CD4 (RPA-T4; BD Biosciences or BioLegend); anti-CCR7 (150503 (R&D Systems) or G043H7 (BioLegend)); anti-CD45RA (H100; eBioscience or BioLegend); and anti-CD57 (TB01; eBioscience). For Phosflow analyses, the following antibodies were used: Alexa Fluor 647–conjugated antibody to AKT

phosphorylated at Ser473 (D9E; Cell Signaling), Alexa Fluor 488–conjugated antibody to AKT phosphorylated at Thr308 (C31E5E; Cell Signaling), phycoerythrin-conjugated antibody to S6 phosphorylated at Ser235 and Ser236 (N7-548; BD Biosciences) and Alexa Fluor 647–conjugated antibody to S6 phosphorylated at Ser240 and Ser244 (D68F8; Cell Signaling). At least three independent experiments were performed.

Cell lysis and immunoblot analysis. Cells were washed in PBS or RPMI medium with no FBS and were immediately lysed in 1%Triton X-100, 50 mM Tris-HCl pH 8, 150 mM NaCl, 2 mM EDTA, 10% glycerol, complete protease inhibitor 'cocktail' (Roche) and phosphatase inhibitor 'cocktails' (Sigma). Lysates were then clarified by centrifugation at 15,000*g* at 4 °C for 10 min and measured for protein content by BCA assay (Pierce). Approximately 20 µg total protein was separated by SDS-PAGE and transferred to a nitrocellulose membrane (Bio-Rad). Nonspecific binding in membranes was blocked for 1 h at 21 °C with 5% nonfat dry milk in Tris-buffered saline (TBS), pH 8.5, with 0.01% Tween-20 (TBST), followed by incubation overnight at 4 °C with primary antibody. After membranes were washed for 1 h at 21 °C with TBST, horseradish peroxidase–conjugated secondary antibody was added for an additional hour at 21 °C. The following validated antibodies were used: anti-p110δ (04-401; Millipore or D1Q7R; Cell Signaling), anti-Myc tag (9B11; Cell Signaling), antibody to AKT phosphorylated at Ser473 (4060; Cell Signaling), anti-AKT (4691; Cell Signaling), goat anti–rabbit IgG (4050; Southern Biotech), goat anti-mouse IgG1 (1070; Southern Biotech) and goat anti–mouse IgG (1030; Southern Biotech). After a final wash step for 1 h, horseradish peroxidase substrate (Clarity; Bio-Rad) was added to the membranes, which were then subjected to chemiluminscence imaging. Band intensities were quantified with Image Lab software (Bio-Rad). The loading control is from stain-free imaging of total protein on the membrane after transfer, focusing on a doublet around 30-35 kDa in size (Bio-Rad).

Protein structure modeling. A model of the structure of p110δ in complex with p85a was generated based on the structure of the p110δ/p85α inter-SH2 complex (PDB:5DXU) (1). Mutations at G124D and E81K were generated in COOT (2), with the most probable rotamer without clashes selected. For G124D no rotamers had an absence of clashes, so the most probable was selected.

Protein expression and purification. The WT PI3K and G124D variant protein complexes were expressed and purified in the same manner, similar to previously described methods (3). Protein complexes were expressed in *Spodoptera frugiperda* (Sf9) cells by co-infecting at 1-2x10^6 cells/mL with an optimized ratio of p110δ:p85α baculovirus. After 40-72 hours, co-infections were harvested by centrifugation before washing with ice-cold PBS and snap-freezing in liquid nitrogen. Protein purifications proceeded at 4°C, and were initiated by re-suspension in lysis buffer (20 mM Tris pH 8.0, 100 mM NaCl, 10 mM imidazole pH 8.0, 5% glycerol (v/v), 2 mM bME, protease inhibitor (Protease Inhibitor Cocktail Set III, Sigma)) before a short sonication protocol (1 min, 15s on, 15s off, level 4.0, Misonix sonicator 3000). Triton X-100 was added (final concentration of 0.1%) prior to lysate being cleared by centrifugation (20,000 g for 45 minutes, Beckman Coulter Avanti J-25I, JA 25.50 rotor), Protein was then purified by nickel affinity by loading the supernatant onto a 5 mL HisTrap™ FF column (GE Healthcare) equilibrated in NiNTA A buffer (20 mM Tris pH 8.0, 100 mM NaCl, 10 mM imidazole pH 8.0, 5% (v/v) glycerol, 2 mM bME) before being washed with 20 mL of NiNTA A

buffer and 6% NiNTA B buffer (20 mM Tris pH 8.0, 100 mM NaCl, 200 mM imidazole pH 8.0, 5% (v/v) glycerol, 2 mM bME). The protein was eluted with 100% NiNTA B buffer, and the eluted protein was further purified by anion exchange. The elution was loaded onto a 5 mL HiTrapTM Q HP column (GE Healthcare) equilibrated in Hep A buffer (20 mM Tris pH 8.0, 100 mM NaCl, 5% (v/v) glycerol, 2 mM bME) and eluted by use of a Hep A buffer and Hep B buffer gradient (20 mM Tris pH 8.0, 1 M NaCl, 5% (v/v) glycerol, 2 mM bME). Fractions containing protein were pooled and concentrated using a 50,000 MWCO Amicon concentrator (Millipore) before purification by size-exclusion chromatography. A Superdex^{TM} 200 10/300 GL Increase size-exclusion column (GE Healthcare) equilibrated in Gel Filtration Buffer (20 mM HEPES pH 7.5, 150 mM NaCl, 0.5 mM tris(2-carboxyethyl)phosphine (TCEP)) was injected with concentrated protein and the eluted protein was concentrated before snap-freezing in liquid nitrogen at 0.5-1.0 mg/mL. Concentrations were determined by measuring absorbance at 280 nm using a NanoDrop (Thermo Scientific).

***In vitro* kinase assays.** Lipid kinase assays monitoring hydrolysis of ATP were carried out using the Transcreener ADP2 FI assay (BellBrook Labs), according to previously published protocols (4). Assays were carried out using lipid vesicles composed of 5% Brain PIP_2, 95% Brain PS (w/v) at a final concentration of 0.45 mg/ml and 100 μM ATP. Experiments with phosphopeptide (mouse PDGFR residues 735–767, with pY740 and pY751) were carried out at a final concentration of 1 μM. *In vitro* lipid kinase activity of PI3K complexes was measured by monitoring ATP hydrolysis using the Transcreener ADP2 Fluorescence Intensity (FI) assay (BellBrook Labs). Proteins were diluted in 2X PI3K kinase buffer (100 mM HEPES pH 7.5, 200 mM NaCl, 6 mM MgCl2, 2 mM EDTA, 0.06% CHAPS, 2 mM TCEP) and reactions were started by the addition of 2X substrate solution (0.9 mg/mL lipid vesicles (5% C8 phosphatidylinositol 4,5 bisphosphate, 95% phosphatidylserine), 200 μM ATP) in a 384-well black microplate (Corning). Reactions were carried out at 23°C for 60 minutes and stopped by addition of 2X Stop and Detect buffer (1X Stop and Detect Buffer, 8 nM ADP Alexa594 Tracer, 93.7 μg/mL ADP2 Antibody-IRDye QC-1). The antibody, tracer and ADP were allowed to equilibrate for 60 minutes before the fluorescence intensity was measured using a Spectramax M5 plate reader ($\lambda_{excitation}$ = 590 nm and $\lambda_{emission}$ = 620 nm; 20 nm bandwidth; Molecular Devices). Calculation of specific activity was performed using an ATP/ADP standard curve according to the Transcreener ADP FI manual and the fold activation was calculated by normalizing all specific activity values to the wild-type PI3K specific activity value. Experiments were performed in triplicate (error shown as SD, n=3).

Hydrogen-deuterium exchange mass spectrometry (HDX-MS). HDX-MS experiments were carried out similar to previously published protocols (5, 6). In brief, initiation of deuterium exchange was carried out by the addition of 45 μL of deuterated buffer (10 mM HEPES pH 7.5, 100 mM NaCl, 98% (v/v) D_2O) and incubated for three different time points (3 s, 30 s, and 300 s at 23°C). The reaction consisted of 50 μL final volume with a PI3K concentration of 120 nM, before being terminated by the addition of 20 μL ice-cold quench buffer (2 M guanidine–HCl, 3% formic acid). Samples were immediately frozen in liquid nitrogen and stored at -80°C.

Protein samples were rapidly thawed and injected onto an online UPLC system for digestion and separation. The protein was run over two immobilized pepsin columns (Applied Biosystems; porosyme, 2-3131-00) at 10°C and 2°C at 200 μL/min for 3 minutes, and peptides were collected onto a VanGuard precolumn trap (Waters). The trap was subsequently eluted in line with an Acquity 1.7 μm particle, 100 × 1 mm2 C18 UPLC column (Waters), using a gradient of 5-36% B (buffer A 0.1% formic acid, buffer B 100% acetonitrile) over 16 minutes. Mass spectrometry experiments were performed on an Impact II TOF (Bruker) acquiring over a mass range from 150 to 2200 m/z using an electrospray ionization source operated at a temperature of 200°C and a spray voltage of 4.5 kV. Peptides were identified using data-dependent acquisition methods following tandem MS/MS experiments (0.5 s precursor scan from 150-2000 m/z; twelve 0.25 s fragment scans from 150-2000 m/z). MS/MS datasets were analyzed using PEAKS7 (PEAKS), and a false discovery rate was set at 1% using a database of purified proteins and known contaminants.

HD-Examiner software (Sierra Analytics) was used to automatically calculate the level of deuterium incorporation into each peptide. All peptides were manually inspected for correct charge state and presence of overlapping peptides. Deuteration levels were calculated using the centroid of the experimental isotope clusters. Results for these proteins are presented as relative levels of deuterium incorporation, and the only control for back exchange was the level of deuterium present in the buffer (78%-PI3K). The real level of deuteration is assumed to be ~25–35% higher than shown, based on tests performed with fully deuterated standard peptides. The average error of all time points and conditions for each HDX project was less than 0.2 Da. Therefore, changes in any peptide at any time point greater than both 7% and 0.7 Da between conditions with a paired t-test value of $p<0.05$ were considered significant. The full deuterium incorporation for all peptides is shown in Fig. E3 and E4.

Statistical analyses

Statistical analysis for differences in lipid kinase activity were carried out using a paired student t-test. For HDX-MS, changes in any peptide at any time point greater than both 7% and 0.7 Da between conditions with a paired t-test value of $p<0.05$ were considered significant. For immunoblot quantification of phospho-AKT (Fig. E5b), indicated p values were from Welch's t test.

Primer sequences

Generation of wild-type PIK3CD expression vector with C-terminal 5xMyc tag.
pcDNA3.1 backbone
Forward: CAGTGTGCTGGAATTCGCCACCATGCCCCCTGGGGTGGACTG
Reverse: TTTTGCTCTGCGGCCGCCTGCCTGTTGTCTTTGGACA

Generation of patient PIK3CD variants by site-directed mutagenesis.
E81K:
Forward: CAGACAGCGGAGCAGCAAAAGCTGGAGGACGAGCAAC
Reverse: GTTGCTCGTCCTCCAGCTTTTGCTGCTCCGCTGTCTG
G124D:
Forward: GCCTCCTCATCGGCAAAGACCTCCACGAGTTTGACTCC
Reverse: GGAGTCAAACTCGTGGAGGTCTTTGCCGATGAGGAGGC

Figure legends

Figure E1. The phenotype of patient lymphocytes. Flow cytometry on PBMCs from a female healthy control subject and patient A.I.1, identifying naive T cells ($CD45RA^+CCR7^+$), central memory T cells ($CD45RA^-CCR7^+$), T_{EM} cells ($CD45RA^-CCR7^-$) and T_{EMRA} cells ($CD45RA^+CCR7^-$). Surface expression on CD4+ and CD8+ lymphocytes of CD27 and CD57 (right) identifying terminally differentiated senescent effector T cells.

Figure E2. Domains and structural analysis of E81 and G124D of p110δ. (a) Schematic of p110δ with previous (black) and novel (red) mutations. (b) E81 and G124 residues (yellow spheres) in the structure of p110δ (PDB 5DXU) with the inter-SH2 domain of p85α (light green). (c) Zoomed-in view of mutant residues with a putative steric clash between G124D and T76 in red.

Figure E3. Summary of all HDX p110δ peptide data. The charge state (Z), residue start (S), residue end number (E), and retention time (RT) are displayed for every peptide. Three timepoints are labelled, and the relative level of HDX is colored on a blue-to-red continuum. Data listed are the average of three independent experiments, with SD given. ## indicates no coverage for the specific peptide.

Figure E4. Summary of all HDX p85α peptide data. The charge state (Z), residue start (S), residue end number (E), and retention time (RT) are displayed for every peptide. Three timepoints are labelled, and the relative level of HDX is colored on a blue-to-red continuum. Data listed are the average of three independent experiments, with SD given. ## indicates no coverage for the specific peptide.

Figure E5. E81K or G124D hyperactivate p110δ despite normal p85 binding. (a) PI3K/AKT/mTOR signaling, adapted from (22). (b) Quantification of phospho-AKT immunoblot data from 5 experiments as in Figure 1e. (c) Phospho-S6 S235/236 or S240/244 in indicated T cell blasts. (d-e) Cumulative data on phospho-AKT S473 and phospho-S6 S240/244 in indicated T cell blasts. (f) p85 immunoprecipitates (IP) or input from healthy T cells overexpressing the indicated protein and probed as indicated.

Supplement References

1. Heffron TP*, et al.* (2016) The Rational Design of Selective Benzoxazepin Inhibitors of the alpha-Isoform of Phosphoinositide 3-Kinase Culminating in the Identification of (S)-2-((2-(1-Isopropyl-1H-1,2,4-triazol-5-yl)-5,6-dihydrobenzo[f]imidazo[1,2-d][1 ,4]oxazepin-9-yl)oxy)propanamide (GDC-0326). *J Med Chem* 59(3):985-1002.
2. Emsley P, Lohkamp B, Scott WG, & Cowtan K (2010) Features and development of Coot. *Acta Crystallogr D Biol Crystallogr* 66(Pt 4):486-501.
3. Burke JE*, et al.* (2011) Dynamics of the phosphoinositide 3-kinase p110delta interaction with p85alpha and membranes reveals aspects of regulation distinct from p110alpha. *Structure* 19(8):1127-1137.
4. Zhang X*, et al.* (2011) Structure of lipid kinase p110beta/p85beta elucidates an unusual SH2-domain-mediated inhibitory mechanism. *Mol Cell* 41(5):567-578.
5. Vadas O, Jenkins, M.L., Dornan, G.L., Burke, J.E. (2016) Chapter Seven - Using Hydrogen-Deuterium Exchange Mass Spectrometry to Examine Protein-Membrane Interactions. *Methods in Enzymology*), Vol 583, pp 143-172.
6. Dornan GL*, et al.* (2017) Conformational disruption of PI3Kδ regulation by immunodeficiency mutations in PIK3CD and PIK3R1. *Proceedings of the National Academy of Sciences* 114(8):1982-1987.
7. Samuels Y*, et al.* (2004) Frequency of Mutations of the PIK3CA Gene in Human Cancers. *Science* 304(5670):554-554.
8. Echeverria I, Liu Y, Gabelli SB, & Amzel LM (2015) Oncogenic mutations weaken the interactions that stabilize the p110α-p85α heterodimer in phosphatidylinositol 3-kinase α. *FEBS Journal* 282(18):3528-3542.
9. Oda K*, et al.* (2008) PIK3CA cooperates with other phosphatidylinositol 3'-kinase pathway mutations to effect oncogenic transformation. *Cancer Res* 68(19):8127-8136.
10. Gymnopoulos M, Elsliger MA, & Vogt PK (2007) Rare cancer-specific mutations in PIK3CA show gain of function. *Proc Natl Acad Sci U S A* 104(13):5569-5574.
11. Ikenoue T*, et al.* (2005) Functional analysis of PIK3CA gene mutations in human colorectal cancer. *Cancer Res* 65(11):4562-4567.
12. Rudd ML*, et al.* (2011) Unique Spectrum of Somatic PIK3CA (p110α) Mutations Within Primary Endometrial Carcinomas. *Clinical Cancer Research* 17(6):1331-1340.
13. Riviere JB*, et al.* (2012) De novo germline and postzygotic mutations in AKT3, PIK3R2 and PIK3CA cause a spectrum of related megalencephaly syndromes. *Nature genetics* 44(8):934-940.
14. Loconte DC*, et al.* (2015) Molecular and Functional Characterization of Three Different Postzygotic Mutations in PIK3CA-Related Overgrowth Spectrum (PROS) Patients: Effects on PI3K/AKT/mTOR Signaling and Sensitivity to PIK3 Inhibitors. *PLoS ONE* 10(4).
15. Mirzaa G*, et al.* (2016) PIK3CA-associated developmental disorders exhibit distinct classes of mutations with variable expression and tissue distribution. *JCI Insight* 1(9).
16. Burke JE, Perisic O, Masson GR, Vadas O, & Williams RL (2012) Oncogenic mutations mimic and enhance dynamic events in the natural activation of phosphoinositide 3-kinase p110alpha (PIK3CA). *Proc Natl Acad Sci U S A* 109(38):15259-15264.
17. Shibata T, Kokubu A, Tsuta K, & Hirohashi S (2009) Oncogenic mutation of PIK3CA in small cell lung carcinoma: a potential therapeutic target pathway for chemotherapy-resistant lung cancer. *Cancer Lett* 283(2):203-211.

18. Lui VWY*, et al.* (2013) Frequent Mutation of the PI3K Pathway in Head and Neck Cancer Defines Predictive Biomarkers. *Cancer Discovery* 3(7):761-769.
19. Rios JJ*, et al.* (2013) Somatic gain-of-function mutations in PIK3CA in patients with macrodactyly. *Hum Mol Genet* 22(3):444-451.
20. Orloff MS*, et al.* (2013) Germline PIK3CA and AKT1 mutations in Cowden and Cowden-like syndromes. *Am J Hum Genet* 92(1):76-80.
21. Ross RL, Askham JM, & Knowles MA (2013) PIK3CA mutation spectrum in urothelial carcinoma reflects cell context-dependent signaling and phenotypic outputs. *Oncogene* 32(6):768-776.
22. Lucas CL*, et al.* (2014) Heterozygous splice mutation in PIK3R1 causes human immunodeficiency with lymphoproliferation due to dominant activation of PI3K. *J Exp Med* 211(13):2537-2547.

Table E1: Extensive clinical table for patients A.I.1, A.II.1, and B.1

	A.I.1	A.II.1	B.1
Amino acid substitution	G124D	G124D	E81K
Presenting symptoms, age of onset	Severe pneumonia, 6 years	CVID/ALPS-like, 0.5 years	Recurrent skin abscesses and pneumonia, failure to thrive, 0.5 years
Viral infections (excluding EBV)	Herpes labialis, warts, herpes zoster	Varicella after vaccine	N.D.
Other bacterial infections	MRSA in BAL, Pseudomonas	Otitis media (x20), bacteremia Strep pneumo, C. diff colitis, bursitis (staph aureus age 4 months)	Y
Fungal infections	Oral candidiasis	Oral candidiasis	N
Splenomegaly	N	Y	N
Pulmonary symptoms and imaging abnormalities	Y lung resection, bronchiectasis	N.D.	PET/CT several confluent peribronchial nodules
Asthma or other allergies	Y	Y	Eczema, asthma -mild persistent
GI symptoms	GERD	N.D.	Abdominal pain
Dermatological abnormalities	Plantar warts	Eczema	Dermatitis
Any other systemic symptoms or signs	Poor dentition	N.D.	Failure to thrive; height and weight <3rd percentile
History of malignancy	N	Abdominal mass	Non-Hodgkin lymphoma but without definitive dx; did not receive chemo or radiation therapy
NK cells (CD3-CD56+CD16+)	74-168/μL ↓ (126-729/μL) 8.3-13.4% (6.2-34.6%)	451/μL (90-900/μL) 13-17% (4-31%)	70-117/μL ↓ (152-595/μL) 6-10% ↓ (7-28%)
Memory B cells (CD27+)	12-21/μL (12-68/μL) 0.8-2.8% (0.8-3.6%)	N.D.	6-22/μL ↓ (19-131/μL) 0.6-1.6% ↓ (1-5%)

Transitional B cells (CD38+IgM+ or CD10+IgM+)	3-9/μL ↓ (9-120/μL) 0.3-0.7% ↓ (0.5-5.3%)	N.D.	160/μL ↑ (0-11/μL) 26.6% ↑ (0-4%)
IgG	462-649 mg/dL ↓ (633-1280 mg/dL) pre-treatment	437-688 mg/dL ↓ (441-1280 mg/dL)	1680-2292 mg/dL ↑ (698-1549 mg/dL)
IgA	27-37 mg/dL) ↓ (33-202 mg/dL) pre-treatment	7-23 mg/dL ↓ (22-202 mg/dL)	N.D.
IgM	157-565 mg/dL ↑ (48-207 mg/dL)	87-413 mg/dL ↑ (47-207 mg/dL)	N.D.
Antibody responsiveness to vaccines	N/A (on Hizentra) Prior to treatment, nl response to pneumococcus, diphtheria toxoid, and tetanus toxoid	Poor response to polysaccharides, tetanus, mumps non-detectable	nl
Lymph node biopsy	Y	N	Y, EBV lymphadenitis, possible benign marginal zone hyperplasia, no lymphoma
Bone marrow biopsy	N.D.	N.D.	Y, normocellular w/trilineage hematopoiesis
Lung biopsy or BAL	Y	N.D.	N.D.
Other surgeries	Lung resection, right salpingo-oophorectomy	Splenectomy, tonsillectomy	Small bowel resection

Abbreviations: ALPS, autoimmune lymphoproliferative syndrome; BAL, bronchoalveolar lavage; CVID, common variable immunodeficiency; dx, diagnosis; EBV, Epstein-Barr virus; GERD, gastroesophageal reflux disease; N, no; N/A, not applicable; N.D., not determined; nl, normal; Y, yes. Numerical data indicate ranges of patient values listed above age-matched reference ranges in parentheses.

Table E2: Reported p110α variants in the ABD and ABD-RBD linker with associated disease phenotypes.

p110α Site	Variant	Cancer Association	PROS Association	Gain-of-Function	Corresponding p110δ Site*
Adaptor-binding domain (AA 16-105)					
R38	C	CR(7)		✔(8, 9)**	*R38*
	H	CR(7)		✔(10, 11)	
E81	K	NEEC(12)	MCAP(13)	✔(14)	*E81*
R88	Q	CR(7), EEC(12), NEEC(12)	MCAP(13)	✔(8, 9, 12)	*R88*
R93	Q	EEC(12)	MCAP(15), OVG(15)	N.D.	Q93
	W	EEC(12)		✔(12)	
P104	L		MCAP(15)	N.D.	R104
	R	CR(7)		N.D.	
ABD-RBD linker (AA 106-186)					
G106	R	EEC(12)		✔(12)	*G106*
	V	CR(7)	OVG(15)	✔(11, 12, 16)	
GNR106	del	SCLC(17)		✔(17)	GDR106
R108	H	NEEC(12)		✔(9)	*R108*
	P	CR(7)		N.D.	
E109	del	EEC(12)		N.D.	V109
E110	K	HNSCC(18)		N.D.	K110
K111	del	CR(7)		✔(12)	*K111*
	E	EEC(12), NEEC(12)		✔(12)	
	N	NEEC(12)		✔(10)	
R115	P		MCAP(15), MD(19)	✔(19)	S115
G118	D	CR(7), EEC(12)	CS(20)	✔(16, 20)	S118
G122	D	CR(7)		N.D.**	*G122*
P124	L	UC(21)		✔(21)	G124
	T	CR(7)		N.D.	
E135	K		CS(20)	N.D.	*E135*
V136	I	UC(21)		N.D.	*V136*

Abbreviations: ABD, adaptor-binding domain; CR, colorectal cancers; CS, Cowden syndrome; EEC, endometrioid endometrial cancer; HNSCC, head and neck squamous cell carcinoma; MCAP, megalencephaly-capillary malformation syndrome; MD, macrodactyly; N.D., not determined; NEEC, non-endometrioid endometrial cancer; OVG, overgrowth; PROS, *PIK3CA*-related overgrowth spectrum; RBD, Ras-binding domain; SCLC, small cell lung cancer; UC, urothelial carcinoma.

*Determined by NCBI Protein BLAST aligning human p110α (P42336.2) with p110δ (O00329.2). Conserved residues are displayed in italics; residues corresponding to mutations in patients A.I.1, A.II.1, or B.1 are in red.

**ExAC browser reports one person each germline heterozygous for minor alleles R38C and G122S (frequency 0.0000083).

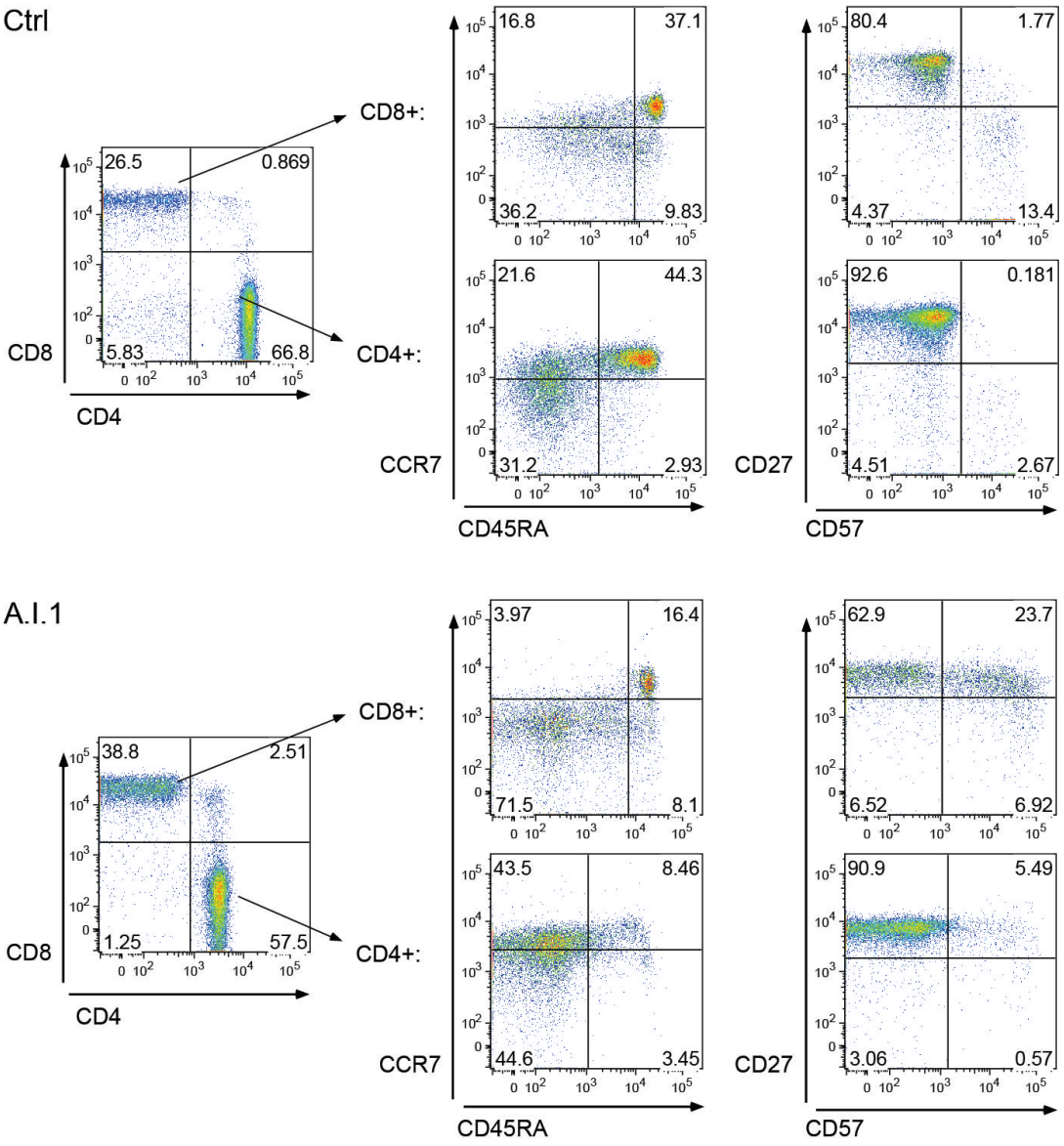
Ctrl
CD8+:
CD4+:
CD8
CD4
CCR7
CD45RA
CD27
CD57
26.5
0.869
5.83
66.8
16.8
37.1
36.2
9.83
21.6
44.3
31.2
2.93
80.4
1.77
4.37
13.4
92.6
0.181
4.51
2.67
A.I.1
38.8
2.51
1.25
57.5
3.97
16.4
71.5
8.1
43.5
8.46
44.6
3.45
62.9
23.7
6.52
6.92
90.9
5.49
3.06
0.57

Figure E1

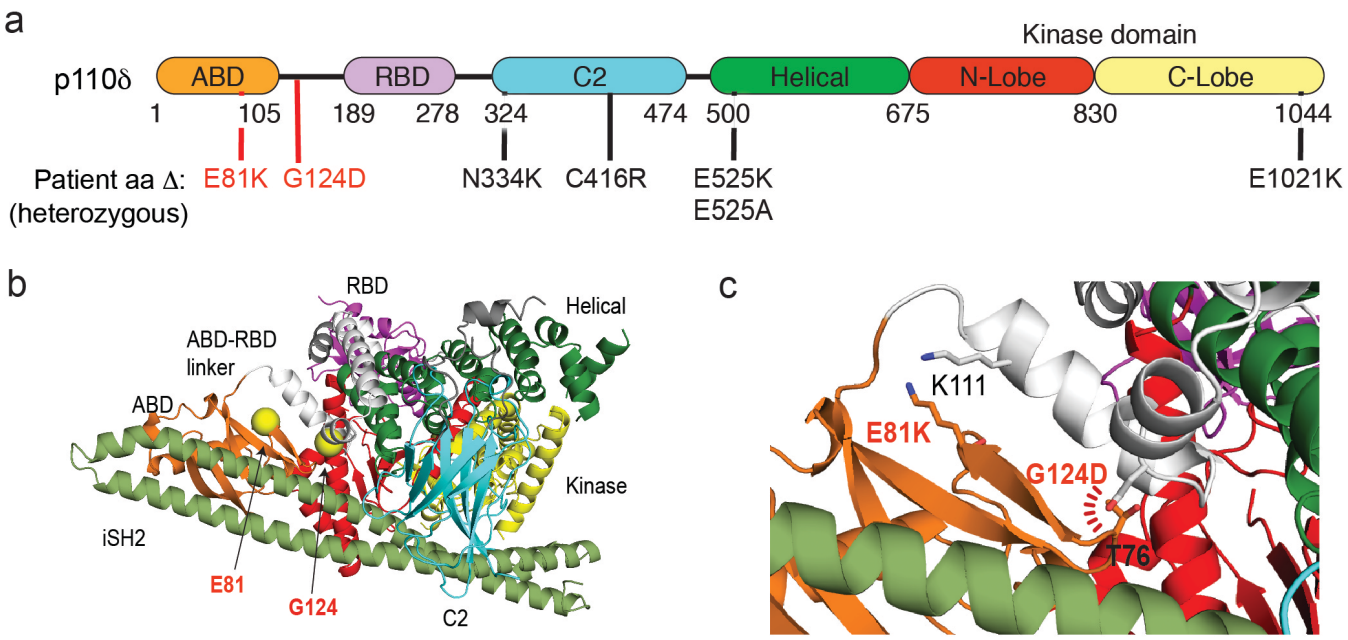
a
Kinase domain
p110δ
ABD
RBD
C2
Helical
N-Lobe
C-Lobe
1
105
189
278
324
474
500
675
830
1044
Patient aa Δ:
(heterozygous)
E81K
G124D
N334K
C416R
E525K
E525A
E1021K
b
RBD
Helical
ABD-RBD
linker
ABD
Kinase
iSH2
E81
G124
C2
c
K111
E81K
G124D
T76

Figure E2

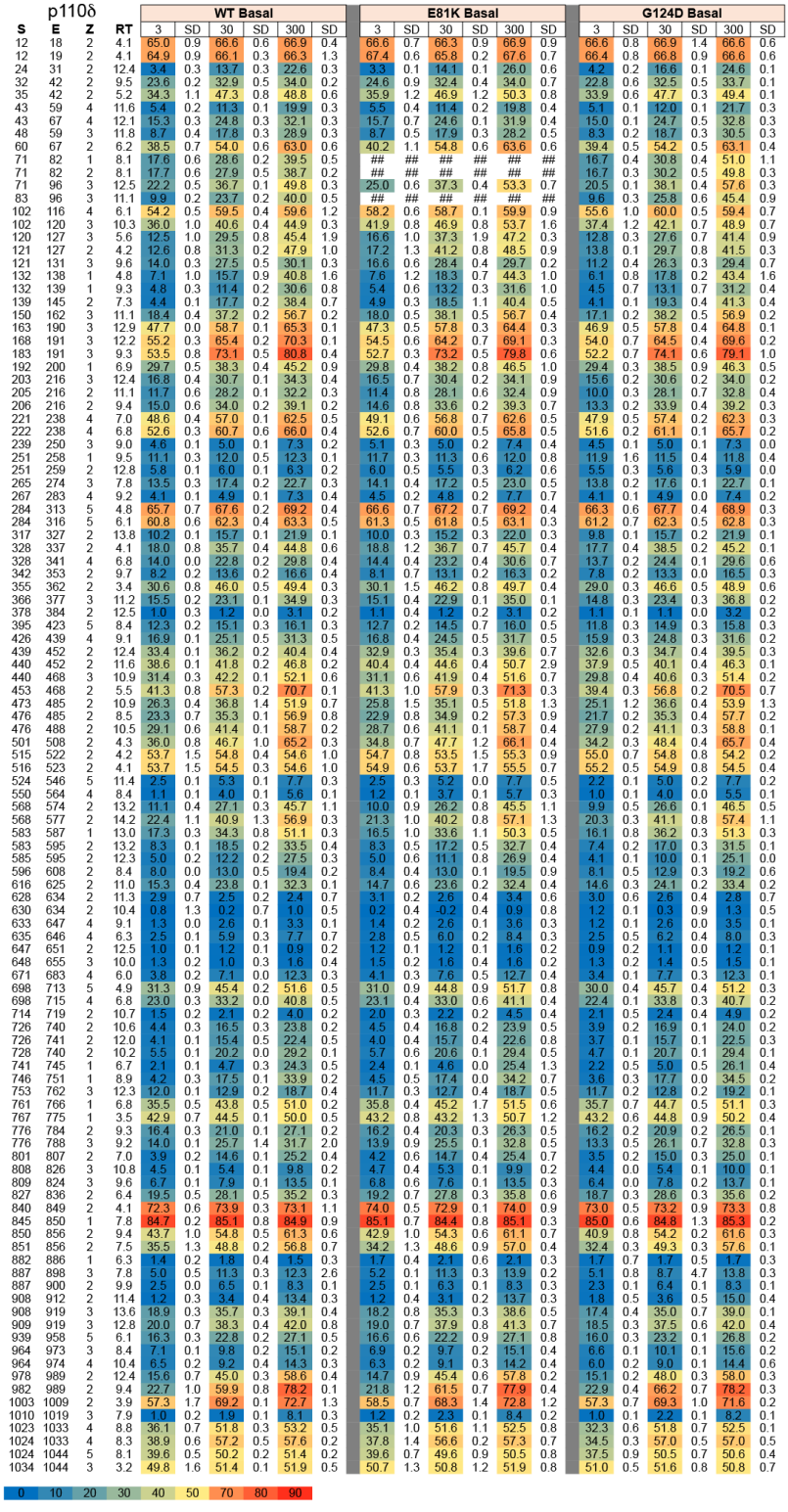

	p110δ			WT Basal						E81K Basal						G124D Basal					
S	E	Z	RT	3	SD	30	SD	300	SD	3	SD	30	SD	300	SD	3	SD	30	SD	300	SD
12	18	2	4.1	65.0	0.9	66.6	0.6	66.9	0.4	66.6	0.7	66.3	0.9	66.9	0.9	66.6	0.8	66.9	1.4	66.6	0.6
12	19	2	4.1	64.9	0.9	66.1	0.3	66.3	1.3	67.4	0.6	65.8	0.2	67.6	0.7	66.4	0.8	66.8	0.9	66.6	0.6
24	31	2	12.4	3.4	0.3	13.7	0.3	22.6	0.3	3.3	0.1	14.1	0.1	26.0	0.6	4.2	0.2	16.6	0.1	24.6	0.1
32	42	2	9.5	23.6	0.2	32.9	0.5	34.0	0.2	24.6	0.9	32.4	0.4	34.0	0.7	22.8	0.6	32.5	0.5	33.7	0.1
35	42	2	5.2	34.3	1.1	47.3	0.8	48.8	0.6	35.9	1.2	46.9	1.2	50.3	0.8	33.9	0.6	47.7	0.3	49.4	0.1
43	59	4	11.6	5.4	0.2	11.3	0.1	19.9	0.3	5.5	0.4	11.4	0.2	19.8	0.4	5.1	0.1	12.0	0.1	21.7	0.3
43	67	4	12.1	15.3	0.3	24.8	0.3	32.1	0.3	15.7	0.7	24.6	0.1	31.9	0.4	15.0	0.1	24.7	0.5	32.8	0.3
48	59	3	11.8	8.7	0.4	17.8	0.3	28.9	0.3	8.7	0.5	17.9	0.3	28.2	0.5	8.3	0.2	18.7	0.3	30.5	0.3
60	67	2	6.2	38.5	0.7	54.0	0.6	63.0	0.6	40.2	1.1	54.8	0.6	63.6	0.6	39.4	0.5	54.2	0.5	63.1	0.4
71	82	1	8.1	17.6	0.6	28.6	0.2	39.5	0.5	##	##	##	##	##	##	16.7	0.4	30.8	0.4	51.0	1.1
71	82	2	8.1	17.7	0.6	27.9	0.5	38.7	0.2	##	##	##	##	##	##	16.7	0.3	30.2	0.5	49.8	0.3
71	96	3	12.5	22.2	0.5	36.7	0.1	49.8	0.3	25.0	0.6	37.3	0.4	53.3	0.7	20.5	0.1	38.1	0.4	57.6	0.3
83	96	3	11.1	9.9	0.2	23.7	0.2	40.0	0.5	##	##	##	##	##	##	9.6	0.3	25.8	0.6	45.4	0.9
102	116	4	6.1	54.2	0.5	59.5	0.4	59.6	1.2	58.2	0.6	58.7	0.1	59.9	0.9	55.6	1.0	60.0	0.5	59.4	0.7
102	120	3	10.3	36.0	1.0	40.6	0.4	44.9	0.3	41.9	0.8	46.9	0.8	53.7	1.6	37.4	1.2	42.1	0.7	48.9	0.7
120	127	3	5.6	12.5	1.0	29.5	0.8	45.4	1.9	16.6	1.0	37.3	1.9	47.2	0.3	12.8	0.3	27.6	0.7	41.4	0.9
121	127	2	4.2	12.6	0.8	31.3	0.2	47.9	1.0	17.2	1.3	41.2	0.8	48.5	0.9	13.8	0.1	29.7	0.8	41.5	0.3
121	131	3	9.6	14.0	0.3	27.5	0.5	30.1	0.3	16.6	0.6	28.4	0.4	29.7	0.2	11.2	0.4	26.3	0.3	29.4	0.7
132	138	1	4.8	7.1	1.0	15.7	0.9	40.8	1.6	7.6	1.2	18.3	0.7	44.3	1.0	6.1	0.8	17.8	0.7	43.4	1.6
132	139	1	9.3	4.8	0.3	11.4	0.2	30.6	0.8	5.4	0.6	13.2	0.3	31.6	1.0	4.5	0.7	13.1	0.7	31.2	0.4
139	145	2	7.3	4.4	0.1	17.7	0.2	38.4	0.7	4.9	0.3	18.5	1.1	40.4	0.5	4.1	0.1	19.3	0.4	41.3	0.4
150	162	3	11.1	18.4	0.4	37.2	0.2	56.7	0.2	18.0	0.5	38.1	0.5	56.7	0.4	17.1	0.2	38.2	0.5	56.9	0.2
163	190	3	12.9	47.7	0.0	58.7	0.1	65.3	0.1	47.3	0.5	57.8	0.3	64.4	0.3	46.9	0.5	57.8	0.4	64.8	0.1
168	191	3	12.2	55.2	0.3	65.4	0.2	70.3	0.1	54.5	0.6	64.2	0.7	69.1	0.3	54.0	0.7	64.5	0.4	69.6	0.2
183	191	3	9.3	53.5	0.8	73.1	0.5	80.8	0.4	52.7	0.3	73.2	0.5	79.8	0.6	52.2	0.7	74.1	0.6	79.1	1.0
192	200	1	6.9	29.7	0.5	38.3	0.4	45.2	0.9	29.8	0.4	38.2	0.8	46.5	1.0	29.4	0.3	38.5	0.9	46.3	0.5
203	216	3	12.4	16.8	0.4	30.7	0.1	34.3	0.4	16.5	0.7	30.4	0.2	34.1	0.9	15.6	0.2	30.6	0.2	34.0	0.2
205	216	2	11.1	11.7	0.6	28.2	0.1	32.2	0.3	11.4	0.8	28.1	0.6	32.4	0.9	10.0	0.3	28.1	0.7	32.8	0.4
206	216	2	9.4	15.0	0.6	34.0	0.2	39.1	0.2	14.6	0.8	33.6	0.2	39.3	0.7	13.3	0.2	33.9	0.4	39.2	0.3
221	238	4	7.0	48.6	0.4	57.0	0.1	62.5	0.5	49.1	0.6	56.8	0.7	62.6	0.5	47.9	0.5	57.4	0.2	62.3	0.3
222	238	4	6.8	52.6	0.3	60.7	0.6	66.0	0.4	52.6	0.7	60.0	0.5	65.8	0.5	51.6	0.2	61.1	0.1	65.7	0.2
239	250	3	9.0	4.6	0.1	5.0	0.1	7.3	0.2	5.1	0.3	5.0	0.2	7.4	0.4	4.5	0.1	5.0	0.1	7.3	0.0
251	258	1	9.5	11.1	0.3	12.0	0.5	12.3	0.1	11.7	0.3	11.3	0.6	12.0	0.8	11.9	1.6	11.5	0.4	11.8	0.4
251	259	2	12.8	5.8	0.1	6.0	0.1	6.3	0.2	6.0	0.5	5.5	0.3	6.2	0.6	5.5	0.3	5.6	0.3	5.9	0.0
265	274	3	7.8	13.5	0.3	17.4	0.2	22.7	0.3	14.1	0.4	17.2	0.5	23.0	0.5	13.8	0.2	17.6	0.1	22.7	0.1
267	283	4	9.2	4.1	0.1	4.9	0.1	7.3	0.4	4.5	0.2	4.8	0.2	7.7	0.7	4.1	0.1	4.9	0.0	7.4	0.2
284	313	5	4.8	65.7	0.7	67.6	0.2	69.2	0.4	66.6	0.7	67.2	0.7	69.2	0.4	66.3	0.6	67.7	0.4	68.9	0.3
284	316	5	6.1	60.8	0.6	62.3	0.4	63.3	0.5	61.3	0.5	61.8	0.5	63.1	0.3	61.2	0.7	62.3	0.5	62.8	0.3
317	327	2	13.8	10.2	0.1	15.7	0.1	21.9	0.1	10.0	0.3	15.2	0.3	22.0	0.3	9.8	0.1	15.7	0.2	21.9	0.1
328	337	2	4.1	18.0	0.8	35.7	0.4	44.8	0.6	18.8	1.2	36.7	0.7	45.7	0.4	17.7	0.4	38.5	0.2	45.2	0.1
328	341	4	6.8	14.0	0.0	22.8	0.2	29.8	0.4	14.4	0.4	23.2	0.4	30.6	0.7	13.7	0.2	24.4	0.1	29.6	0.6
342	353	2	9.7	8.2	0.2	13.6	0.2	16.6	0.4	8.1	0.7	13.1	0.2	16.3	0.2	7.8	0.2	13.3	0.0	16.5	0.3
355	362	2	3.4	30.6	0.8	46.0	0.5	49.4	0.3	30.1	1.5	46.2	0.8	49.7	0.4	29.0	0.3	46.6	0.5	48.9	0.6
366	377	3	11.2	15.5	0.2	23.1	0.1	34.9	0.3	15.1	0.4	22.9	0.1	35.0	0.1	14.8	0.3	23.4	0.3	36.8	0.2
378	384	2	12.5	1.0	0.3	1.2	0.0	3.1	0.2	1.1	0.4	1.2	0.2	3.1	0.2	1.1	0.1	1.1	0.0	3.2	0.2
395	423	5	8.4	12.3	0.2	15.1	0.3	16.1	0.3	12.7	0.2	14.5	0.7	16.0	0.5	11.8	0.3	14.9	0.3	15.8	0.3
426	439	4	9.1	16.9	0.1	25.1	0.5	31.3	0.5	16.8	0.4	24.5	0.5	31.7	0.5	15.9	0.3	24.8	0.3	31.6	0.2
439	452	2	12.4	33.4	0.1	36.2	0.2	40.4	0.4	32.9	0.3	35.4	0.3	39.6	0.7	32.6	0.3	34.7	0.4	39.5	0.3
440	452	2	11.6	38.6	0.1	41.8	0.2	46.8	0.2	40.4	0.4	44.6	0.4	50.7	2.9	37.9	0.5	40.1	0.4	46.3	0.1
440	468	3	10.9	31.4	0.3	42.2	0.1	52.1	0.6	31.1	0.6	41.9	0.4	51.6	0.7	29.8	0.4	40.6	0.3	51.4	0.2
453	468	2	5.5	41.3	0.8	57.3	0.2	70.7	0.1	41.3	1.0	57.9	0.3	71.3	0.3	39.4	0.3	56.8	0.2	70.5	0.7
473	485	2	10.9	26.3	0.4	36.8	1.4	51.9	0.7	25.8	1.5	35.1	0.5	51.8	1.3	25.1	1.2	36.6	0.4	53.9	1.3
476	485	2	8.5	23.3	0.7	35.3	0.1	56.9	0.8	22.9	0.8	34.9	0.2	57.3	0.9	21.7	0.2	35.3	0.4	57.7	0.2
476	488	2	10.5	29.1	0.6	41.4	0.1	58.7	0.2	28.7	0.6	41.1	0.1	58.7	0.4	27.9	0.2	41.1	0.3	58.8	0.1
501	508	2	4.3	36.0	0.8	46.7	1.0	65.2	0.3	34.8	0.7	47.7	1.2	66.1	0.4	34.2	0.3	48.4	0.4	65.7	0.4
515	522	2	4.2	53.7	1.5	54.8	0.4	54.6	1.0	54.7	0.8	53.5	1.5	55.3	0.9	55.0	0.7	54.8	0.8	54.2	0.2
516	523	2	4.1	53.7	1.5	54.5	0.3	54.6	1.0	54.9	0.6	53.7	1.7	55.5	0.7	55.2	0.5	54.9	0.8	54.5	0.4
524	546	5	11.4	2.5	0.1	5.3	0.1	7.7	0.3	2.5	0.3	5.2	0.0	7.7	0.5	2.2	0.1	5.0	0.2	7.7	0.2
550	564	4	8.4	1.1	0.1	4.0	0.1	5.6	0.1	1.2	0.1	3.7	0.1	5.7	0.3	1.0	0.1	4.0	0.0	5.5	0.1
568	574	2	13.2	11.1	0.4	27.1	0.3	45.7	1.1	10.0	0.9	26.2	0.8	45.5	1.1	9.9	0.5	26.6	0.1	46.5	0.5
568	577	2	14.2	22.4	1.1	40.9	1.3	56.9	0.3	21.3	1.0	40.2	0.8	57.1	1.3	20.3	0.3	41.1	0.8	57.4	1.1
583	587	1	13.0	17.3	0.3	34.3	0.8	51.1	0.3	16.5	1.0	33.6	1.1	50.3	0.5	16.1	0.8	36.2	0.3	51.3	0.3
583	595	2	13.2	8.3	0.1	18.5	0.2	33.5	0.4	8.3	0.5	17.2	0.5	32.7	0.4	7.4	0.2	17.0	0.3	31.5	0.1
585	595	2	12.3	5.0	0.2	12.2	0.2	27.5	0.3	5.0	0.6	11.1	0.8	26.9	0.4	4.1	0.1	10.0	0.1	25.1	0.0
596	608	2	8.4	8.0	0.0	13.0	0.5	19.4	0.2	8.4	0.4	13.0	0.1	19.5	0.9	8.1	0.5	12.9	0.3	19.2	0.6
616	625	2	11.0	15.3	0.4	23.8	0.1	32.3	0.1	14.7	0.6	23.6	0.2	32.4	0.4	14.6	0.3	24.1	0.2	33.4	0.2
628	634	2	11.3	2.9	0.7	2.5	0.2	2.4	0.7	3.1	0.2	2.6	0.4	3.4	0.6	3.0	0.6	2.6	0.4	2.8	0.7
630	634	2	10.4	0.8	1.3	0.2	0.7	1.0	0.5	0.2	0.4	-0.2	0.4	0.9	0.8	1.2	0.1	0.3	0.9	1.3	0.5
633	647	4	9.1	1.3	0.0	2.6	0.1	3.3	0.1	1.4	0.2	2.6	0.1	3.6	0.3	1.2	0.1	2.6	0.0	3.5	0.1
635	646	4	6.3	2.5	0.1	5.9	0.3	7.7	0.7	2.8	0.5	6.0	0.2	8.4	0.3	2.5	0.5	6.2	0.4	8.0	0.3
647	651	2	12.5	1.0	0.1	1.2	0.1	0.9	0.2	1.2	0.1	1.2	0.1	1.6	0.2	0.9	0.2	1.1	0.0	1.2	0.1
648	655	3	10.0	1.3	0.2	1.0	0.3	1.6	0.4	1.5	0.2	1.6	0.4	1.6	0.2	1.3	0.2	1.4	0.5	1.5	0.1
671	683	4	6.0	3.8	0.2	7.1	0.0	12.3	0.3	4.1	0.3	7.6	0.5	12.7	0.4	3.4	0.1	7.7	0.3	12.3	0.1
698	713	5	4.9	31.3	0.9	45.4	0.2	51.6	0.5	31.0	0.9	44.8	0.9	51.7	0.8	30.0	0.4	45.7	0.4	51.2	0.3
698	715	4	6.8	23.0	0.3	33.2	0.0	40.8	0.5	23.1	0.4	33.0	0.6	41.1	0.4	22.4	0.1	33.8	0.3	40.7	0.2
714	719	2	10.7	1.5	0.2	2.1	0.2	4.0	0.2	2.0	0.3	2.2	0.2	4.5	0.4	2.1	0.5	2.4	0.4	4.9	0.2
726	740	2	10.6	4.4	0.3	16.5	0.3	23.8	0.2	4.5	0.4	16.8	0.2	23.9	0.5	3.9	0.2	16.9	0.1	24.0	0.2
726	741	2	12.0	4.1	0.1	15.4	0.5	22.4	0.5	4.0	0.4	15.7	0.4	22.6	0.8	3.7	0.1	15.7	0.1	22.5	0.3
728	740	2	10.2	5.5	0.1	20.2	0.0	29.2	0.1	5.7	0.6	20.6	0.1	29.4	0.5	4.7	0.1	20.7	0.1	29.4	0.1
741	745	1	6.7	2.1	0.1	4.7	0.3	24.3	0.5	2.4	0.1	4.6	0.0	25.4	1.3	2.2	0.5	5.0	0.5	26.1	0.4
746	751	1	8.9	4.2	0.3	17.5	0.1	33.9	0.2	4.5	0.5	17.4	0.0	34.2	0.7	3.6	0.3	17.7	0.0	34.5	0.2
753	762	3	12.3	12.0	0.1	12.9	0.2	18.7	0.4	11.7	0.3	12.7	0.4	18.7	0.5	11.7	0.2	12.8	0.2	19.2	0.1
761	766	1	6.8	35.5	0.5	43.8	0.5	51.0	0.2	35.8	0.4	45.2	1.7	51.5	0.6	35.7	0.7	44.7	0.5	51.1	0.3
767	775	1	3.5	42.9	0.7	44.5	0.1	50.0	0.5	43.2	0.8	43.2	1.3	50.7	1.2	43.2	0.6	44.8	0.9	50.2	0.4
776	784	2	9.3	16.4	0.3	21.0	0.1	27.1	0.2	16.2	0.4	20.3	0.3	26.3	0.5	16.2	0.2	20.9	0.2	26.5	0.1
776	788	3	9.2	14.0	0.1	25.7	1.4	31.7	2.0	13.9	0.9	25.5	0.1	32.8	0.5	13.3	0.5	26.1	0.7	32.8	0.3
801	807	2	7.0	3.9	0.2	14.6	0.1	25.2	0.4	4.2	0.6	14.7	0.4	25.4	0.7	3.5	0.2	15.0	0.3	25.0	0.1
808	826	3	10.8	4.5	0.1	5.4	0.1	9.8	0.2	4.7	0.4	5.3	0.1	9.9	0.2	4.4	0.0	5.4	0.1	10.0	0.1
809	824	3	9.6	6.7	0.1	7.9	0.1	13.5	0.1	6.8	0.6	7.6	0.1	13.5	0.3	6.4	0.0	7.8	0.2	13.7	0.1
827	836	2	6.4	19.5	0.5	28.1	0.5	35.2	0.3	19.2	0.7	27.8	0.3	35.8	0.6	18.7	0.3	28.6	0.3	35.6	0.2
840	849	2	4.1	72.3	0.6	73.9	0.3	73.1	1.1	74.0	0.5	72.9	0.1	74.0	0.9	73.0	0.5	73.2	0.9	73.3	0.8
845	856	1	7.8	84.7	0.2	85.1	0.8	84.9	0.3	85.1	0.7	84.4	0.3	85.1	0.3	85.0	0.6	84.8	1.2	85.3	0.2
850	856	2	9.4	43.7	1.0	54.8	0.5	61.3	0.6	42.9	1.0	54.3	0.6	61.1	0.7	40.9	0.8	54.2	0.2	61.6	0.3
851	856	2	7.5	35.5	1.3	48.8	0.2	56.8	0.7	34.2	1.3	48.6	0.9	57.0	0.4	32.4	0.3	49.3	0.3	57.6	0.1
882	886	1	6.3	1.4	0.2	1.8	0.4	1.5	0.3	1.7	0.4	2.1	0.6	2.1	0.3	1.7	0.7	1.7	0.5	1.7	0.3
887	898	3	7.8	5.0	0.5	11.3	0.3	12.3	2.6	5.2	0.1	11.3	0.3	13.9	0.2	5.1	0.8	8.7	4.7	13.8	0.3
887	900	2	9.9	2.5	0.0	6.5	0.1	8.3	0.1	2.5	0.1	6.3	0.1	8.3	0.3	2.3	0.1	6.4	0.1	8.3	0.1
908	912	2	11.4	1.2	0.3	3.4	0.4	13.4	0.3	1.2	0.4	3.1	0.2	13.7	0.3	1.8	0.5	3.6	0.5	15.0	0.4
908	919	3	13.6	18.9	0.3	35.7	0.3	39.1	0.4	18.2	0.8	35.3	0.3	38.6	0.5	17.4	0.4	35.0	0.7	39.0	0.1
909	919	3	12.8	20.0	0.7	38.3	0.4	42.0	0.8	19.0	0.7	37.9	0.8	41.3	0.7	18.5	0.3	37.5	0.6	42.0	0.4
939	958	5	6.1	16.3	0.3	22.8	0.2	27.1	0.5	16.6	0.6	22.2	0.9	27.1	0.8	16.0	0.3	23.2	0.1	26.8	0.2
964	973	3	8.4	7.1	0.1	9.8	0.2	15.1	0.2	6.9	0.2	9.7	0.2	15.1	0.4	6.6	0.1	10.1	0.1	15.6	0.2
964	974	4	10.4	6.5	0.2	9.2	0.4	14.3	0.3	6.3	0.2	9.1	0.3	14.2	0.4	6.0	0.2	9.0	0.1	14.4	0.6
978	989	2	12.4	15.6	0.7	45.0	0.3	58.6	0.4	14.7	0.9	45.4	0.6	57.8	0.2	15.1	0.2	48.0	0.3	58.0	0.3
982	989	2	9.4	22.7	1.0	59.9	0.8	78.2	0.1	21.8	1.2	61.5	0.7	77.9	0.4	22.9	0.4	66.2	0.7	78.2	0.3
1003	1009	2	3.9	57.3	1.7	69.2	0.1	72.7	1.3	58.5	0.7	68.3	1.4	72.8	1.2	57.3	0.7	69.3	1.0	71.6	0.2
1010	1019	3	7.9	1.0	0.2	1.9	0.1	8.1	0.3	1.2	0.2	2.3	0.1	8.4	0.2	1.0	0.1	2.2	0.1	8.2	0.1
1023	1033	4	8.8	36.1	0.7	51.8	0.3	53.2	0.5	35.1	1.0	51.6	1.1	52.5	0.8	32.3	0.6	51.8	0.7	52.5	0.1
1024	1033	4	8.3	38.9	0.6	57.2	0.5	57.6	0.2	37.8	1.4	56.6	0.2	57.3	0.7	34.5	0.3	57.0	0.5	57.0	0.5
1024	1044	5	8.1	39.6	0.5	50.2	0.2	51.4	0.2	39.6	0.7	49.6	0.9	50.5	0.8	37.5	0.9	50.5	0.7	50.6	0.4
1034	1044	3	3.2	49.8	1.6	51.4	0.1	51.9	0.5	50.7	1.3	50.8	1.2	51.9	0.8	51.0	0.5	51.6	0.8	50.8	0.7

0 10 20 30 40 50 70 80 90

Figure E3

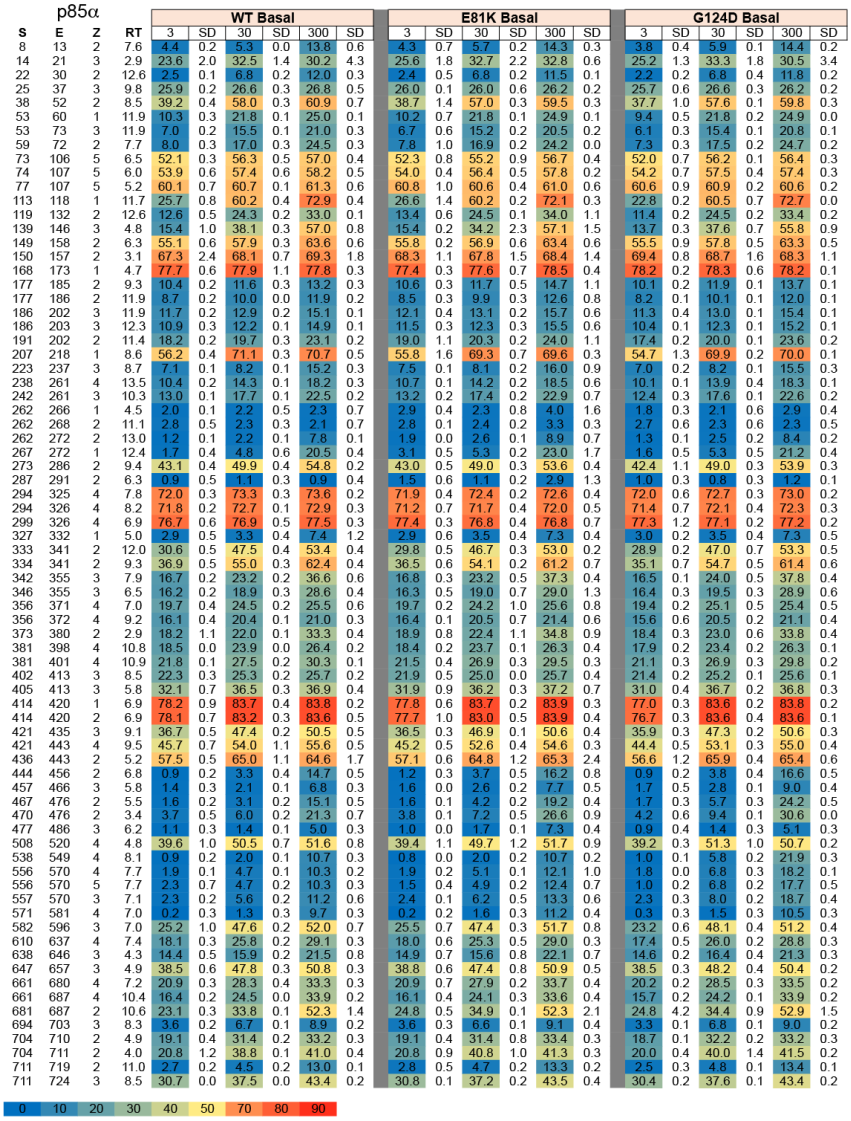

p85α				WT Basal						E81K Basal						G124D Basal					
S	E	Z	RT	3	SD	30	SD	300	SD	3	SD	30	SD	300	SD	3	SD	30	SD	300	SD
8	13	2	7.6	4.4	0.2	5.3	0.0	13.8	0.6	4.3	0.7	5.7	0.2	14.3	0.3	3.8	0.4	5.9	0.1	14.4	0.2
14	21	3	2.9	23.6	2.0	32.5	1.4	30.2	4.3	25.6	1.8	32.7	2.2	32.8	0.6	25.2	1.3	33.3	1.8	30.5	3.4
22	30	2	12.6	2.5	0.1	6.8	0.2	12.0	0.3	2.4	0.5	6.8	0.2	11.5	0.1	2.2	0.2	6.8	0.4	11.8	0.2
25	37	3	9.8	25.9	0.2	26.6	0.3	26.8	0.5	26.0	0.1	26.0	0.6	26.2	0.2	25.7	0.6	26.6	0.3	26.2	0.2
38	52	2	8.5	39.2	0.4	58.0	0.3	60.9	0.7	38.7	1.4	57.0	0.3	59.5	0.3	37.7	1.0	57.6	0.1	59.8	0.3
53	60	1	11.9	10.3	0.3	21.8	0.1	25.0	0.1	10.2	0.7	21.8	0.1	24.9	0.1	9.4	0.5	21.8	0.2	24.9	0.0
53	73	3	11.9	7.0	0.2	15.5	0.1	21.0	0.3	6.7	0.6	15.2	0.2	20.5	0.2	6.1	0.3	15.4	0.1	20.8	0.1
59	72	2	7.7	8.0	0.3	17.0	0.3	24.5	0.3	7.8	1.0	16.9	0.2	24.2	0.0	7.3	0.3	17.5	0.2	24.7	0.2
73	106	5	6.5	52.1	0.3	56.3	0.5	57.0	0.4	52.3	0.8	55.2	0.9	56.7	0.4	52.0	0.7	56.2	0.1	56.4	0.3
74	107	5	6.0	53.9	0.6	57.4	0.6	58.2	0.5	54.0	0.4	56.4	0.5	57.8	0.2	54.2	0.7	57.5	0.4	57.4	0.3
77	107	5	5.2	60.1	0.7	60.7	0.1	61.3	0.6	60.8	1.0	60.6	0.4	61.0	0.6	60.6	0.9	60.9	0.2	60.6	0.2
113	118	1	11.7	25.7	0.8	60.2	0.4	72.9	0.4	26.6	1.4	60.2	0.2	72.1	0.3	22.8	0.2	60.5	0.7	72.7	0.0
119	132	2	12.6	12.6	0.5	24.3	0.2	33.0	0.1	13.4	0.6	24.5	0.1	34.0	1.1	11.4	0.2	24.5	0.2	33.4	0.2
139	146	3	4.8	15.4	1.0	38.1	0.3	57.0	0.8	15.4	0.2	34.2	2.3	57.1	1.5	13.7	0.3	37.6	0.7	55.8	0.9
149	158	2	6.3	55.1	0.6	57.9	0.3	63.6	0.6	55.8	0.2	56.9	0.6	63.4	0.6	55.5	0.9	57.8	0.5	63.3	0.5
150	157	2	3.1	67.3	2.4	68.1	0.7	69.3	1.8	68.3	1.1	67.8	1.5	68.4	1.4	69.4	0.8	68.7	1.6	68.3	1.1
168	173	1	4.7	77.7	0.6	77.9	1.1	77.8	0.3	77.4	0.3	77.6	0.7	78.5	0.4	78.2	0.2	78.3	0.6	78.2	0.1
177	185	2	9.3	10.4	0.2	11.6	0.3	13.2	0.3	10.6	0.3	11.7	0.5	14.7	1.1	10.1	0.2	11.9	0.1	13.7	0.1
177	186	2	11.9	8.7	0.2	10.0	0.0	11.9	0.2	8.5	0.3	9.9	0.3	12.6	0.8	8.2	0.1	10.1	0.1	12.0	0.1
186	202	3	11.9	11.7	0.2	12.9	0.2	15.1	0.1	12.1	0.4	13.1	0.2	15.7	0.6	11.3	0.4	13.0	0.1	15.4	0.1
186	203	3	12.3	10.9	0.3	12.2	0.1	14.9	0.1	11.5	0.3	12.3	0.3	15.5	0.6	10.4	0.1	12.3	0.1	15.2	0.1
191	202	2	11.4	18.2	0.2	19.7	0.3	23.1	0.2	19.0	1.1	20.3	0.2	24.0	1.1	17.4	0.2	20.0	0.1	23.6	0.2
207	218	1	8.6	56.2	0.4	71.1	0.3	70.7	0.5	55.8	1.6	69.3	0.7	69.6	0.3	54.7	1.3	69.9	0.2	70.0	0.1
223	237	3	8.7	7.1	0.1	8.2	0.1	15.2	0.3	7.5	0.1	8.1	0.2	16.0	0.9	7.0	0.2	8.2	0.1	15.5	0.3
238	261	4	13.5	10.4	0.2	14.3	0.1	18.2	0.3	10.7	0.1	14.2	0.2	18.5	0.6	10.1	0.1	13.9	0.4	18.3	0.1
242	261	3	10.3	13.0	0.1	17.7	0.1	22.5	0.2	13.2	0.2	17.4	0.2	22.9	0.7	12.4	0.3	17.6	0.1	22.6	0.2
262	266	1	4.5	2.0	0.1	2.2	0.5	2.3	0.7	2.9	0.4	2.3	0.8	4.0	1.6	1.8	0.3	2.1	0.6	2.9	0.4
262	268	2	11.1	2.8	0.5	2.3	0.3	2.1	0.7	2.8	0.1	2.4	0.2	3.3	0.3	2.7	0.6	2.3	0.6	2.3	0.5
262	272	2	13.0	1.2	0.1	2.2	0.1	7.8	0.1	1.9	0.0	2.6	0.1	8.9	0.7	1.3	0.1	2.5	0.2	8.4	0.2
267	272	1	12.4	1.7	0.4	4.8	0.6	20.5	0.4	3.1	0.5	5.3	0.2	23.0	1.7	1.6	0.5	5.3	0.5	21.2	0.4
273	286	2	9.4	43.1	0.4	49.9	0.4	54.8	0.2	43.0	0.5	49.0	0.3	53.6	0.4	42.4	1.1	49.0	0.3	53.9	0.3
287	291	2	6.3	0.9	0.5	1.1	0.3	0.9	0.4	1.5	0.6	1.1	0.2	2.9	1.3	1.0	0.3	0.8	0.3	1.2	0.1
294	325	4	7.8	72.0	0.3	73.3	0.3	73.6	0.2	71.9	0.4	72.4	0.2	72.6	0.4	72.0	0.6	72.7	0.3	73.0	0.2
294	326	4	8.2	71.8	0.2	72.7	0.1	72.9	0.3	71.2	0.7	71.7	0.4	72.0	0.5	71.4	0.7	72.1	0.4	72.3	0.3
299	326	4	6.9	76.7	0.6	76.9	0.5	77.5	0.3	77.4	0.3	76.8	0.4	76.8	0.7	77.3	1.2	77.1	0.2	77.2	0.2
327	332	1	5.0	2.9	0.5	3.3	0.4	7.4	1.2	2.9	0.6	3.5	0.4	7.3	0.4	3.0	0.2	3.5	0.4	7.3	0.5
333	341	2	12.0	30.6	0.5	47.5	0.4	53.4	0.4	29.8	0.5	46.7	0.3	53.0	0.2	28.9	0.2	47.0	0.7	53.3	0.5
334	341	2	9.3	36.9	0.5	55.0	0.3	62.4	0.4	36.5	0.6	54.1	0.2	61.2	0.7	35.1	0.7	54.7	0.5	61.4	0.6
342	355	3	7.9	16.7	0.2	23.2	0.2	36.6	0.6	16.8	0.3	23.2	0.5	37.3	0.4	16.5	0.1	24.0	0.5	37.8	0.4
346	355	3	6.5	16.2	0.2	18.9	0.3	28.6	0.4	16.3	0.5	19.0	0.7	29.0	1.3	16.4	0.3	19.5	0.3	28.9	0.6
356	371	4	7.0	19.7	0.4	24.5	0.2	25.5	0.6	19.7	0.2	24.2	1.0	25.6	0.8	19.4	0.2	25.1	0.5	25.4	0.5
356	372	4	9.2	16.1	0.4	20.4	0.1	21.0	0.3	16.4	0.1	20.5	0.7	21.4	0.6	15.6	0.6	20.5	0.2	21.1	0.4
373	380	2	2.9	18.2	1.1	22.0	0.1	33.3	0.4	18.9	0.8	22.4	1.1	34.8	0.9	18.4	0.3	23.0	0.6	33.8	0.4
381	398	4	10.8	18.5	0.0	23.9	0.0	26.4	0.2	18.4	0.2	23.7	0.1	26.3	0.4	17.9	0.2	23.4	0.2	26.3	0.1
381	401	4	10.9	21.8	0.1	27.5	0.2	30.3	0.1	21.5	0.4	26.9	0.3	29.5	0.3	21.1	0.3	26.9	0.3	29.8	0.2
402	413	3	8.5	22.3	0.3	25.3	0.2	25.7	0.2	21.9	0.5	25.0	0.0	25.7	0.4	21.4	0.2	25.2	0.1	25.6	0.1
405	413	3	5.8	32.1	0.7	36.5	0.3	36.9	0.4	31.9	0.9	36.2	0.3	37.2	0.7	31.0	0.4	36.7	0.2	36.8	0.3
414	420	1	6.9	78.2	0.9	83.7	0.4	83.8	0.2	77.8	0.6	83.7	0.2	83.9	0.3	77.0	0.3	83.6	0.2	83.8	0.2
414	420	2	6.9	78.1	0.7	83.2	0.3	83.6	0.5	77.7	1.0	83.0	0.5	83.9	0.4	76.7	0.3	83.6	0.4	83.6	0.1
421	435	3	9.1	36.7	0.5	47.4	0.2	50.5	0.5	36.5	0.3	46.9	0.1	50.6	0.4	35.9	0.3	47.3	0.2	50.6	0.3
421	443	4	9.5	45.7	0.7	54.0	1.1	55.6	0.5	45.2	0.5	52.6	0.4	54.6	0.3	44.4	0.5	53.1	0.3	55.0	0.4
436	443	2	5.2	57.5	0.5	65.0	1.1	64.6	1.7	57.1	0.6	64.8	1.2	65.3	2.4	56.6	1.2	65.9	0.4	65.4	0.6
444	456	2	6.8	0.9	0.2	3.3	0.4	14.7	0.5	1.2	0.3	3.7	0.5	16.2	0.8	0.9	0.2	3.8	0.4	16.6	0.5
457	466	3	5.8	1.4	0.3	2.1	0.1	6.8	0.3	1.6	0.0	2.6	0.2	7.7	0.5	1.7	0.5	2.8	0.1	9.0	0.4
467	476	2	5.5	1.6	0.2	3.1	0.2	15.1	0.5	1.6	0.1	4.2	0.2	19.2	0.4	1.7	0.3	5.7	0.3	24.2	0.5
470	476	2	3.4	3.7	0.5	6.0	0.2	21.3	0.7	3.8	0.1	7.2	0.5	26.6	0.9	4.2	0.6	9.4	0.1	30.6	0.0
477	486	3	6.2	1.1	0.3	1.4	0.1	5.0	0.3	1.0	0.0	1.7	0.1	7.3	0.4	0.9	0.4	1.4	0.3	5.1	0.3
508	520	4	4.8	39.6	1.0	50.5	0.7	51.6	0.8	39.4	1.1	49.7	1.2	51.7	0.9	39.2	0.3	51.3	1.0	50.7	0.2
538	549	4	8.1	0.9	0.2	2.0	0.1	10.7	0.3	0.8	0.0	2.0	0.2	10.7	0.2	1.0	0.1	5.8	0.2	21.9	0.3
556	570	4	7.7	1.9	0.1	4.7	0.1	10.3	0.2	1.9	0.2	5.1	0.1	12.1	1.0	1.8	0.0	6.8	0.3	18.2	0.1
556	570	5	7.7	2.3	0.7	4.7	0.2	10.3	0.3	1.5	0.4	4.9	0.2	12.4	0.7	1.0	0.2	6.8	0.2	17.7	0.5
557	570	3	7.1	2.3	0.2	5.6	0.2	11.2	0.6	2.4	0.1	6.2	0.5	13.3	0.6	2.3	0.3	8.0	0.2	18.7	0.4
571	581	4	7.0	0.2	0.3	1.3	0.3	9.7	0.3	0.2	0.2	1.6	0.3	11.2	0.4	0.3	0.3	1.5	0.3	10.5	0.3
582	596	3	7.0	25.2	1.0	47.6	0.2	52.0	0.7	25.5	0.7	47.4	0.3	51.7	0.8	23.2	0.6	48.1	0.4	51.2	0.4
610	637	4	7.4	18.1	0.3	25.8	0.2	29.1	0.3	18.0	0.6	25.3	0.5	29.0	0.3	17.4	0.5	26.0	0.2	28.8	0.3
638	646	3	4.3	14.4	0.5	15.9	0.2	21.5	0.8	14.9	0.7	15.6	0.8	22.1	0.7	14.6	0.2	16.4	0.4	21.3	0.3
647	657	3	4.9	38.5	0.6	47.8	0.3	50.8	0.3	38.8	0.6	47.4	0.8	50.9	0.5	38.5	0.3	48.2	0.4	50.4	0.2
661	680	4	7.2	20.9	0.3	28.3	0.4	33.3	0.3	20.9	0.7	27.9	0.2	33.7	0.4	20.2	0.2	28.5	0.3	33.5	0.2
661	687	4	10.4	16.4	0.2	24.5	0.0	33.9	0.2	16.1	0.4	24.1	0.3	33.6	0.4	15.7	0.2	24.2	0.1	33.9	0.2
681	687	2	10.6	23.1	0.3	33.8	0.1	52.3	1.4	24.8	0.5	34.9	0.1	52.3	2.1	24.8	4.2	34.4	0.9	52.9	1.5
694	703	3	8.3	3.6	0.2	6.7	0.1	8.9	0.2	3.6	0.3	6.6	0.1	9.1	0.4	3.3	0.1	6.8	0.1	9.0	0.2
704	710	2	4.9	19.1	0.4	31.4	0.2	33.2	0.3	19.1	0.4	31.4	0.8	33.4	0.3	18.7	0.1	32.2	0.2	33.2	0.3
704	711	2	4.0	20.8	1.2	38.8	0.1	41.0	0.4	20.8	0.9	40.8	1.0	41.3	0.3	20.0	0.4	40.0	1.4	41.5	0.2
711	719	2	11.0	2.7	0.2	4.5	0.2	13.0	0.1	2.8	0.5	4.7	0.2	13.3	0.2	2.5	0.3	4.8	0.1	13.4	0.1
711	724	3	8.5	30.7	0.0	37.5	0.0	43.4	0.2	30.8	0.1	37.2	0.2	43.5	0.4	30.4	0.2	37.6	0.1	43.4	0.2

Figure E4

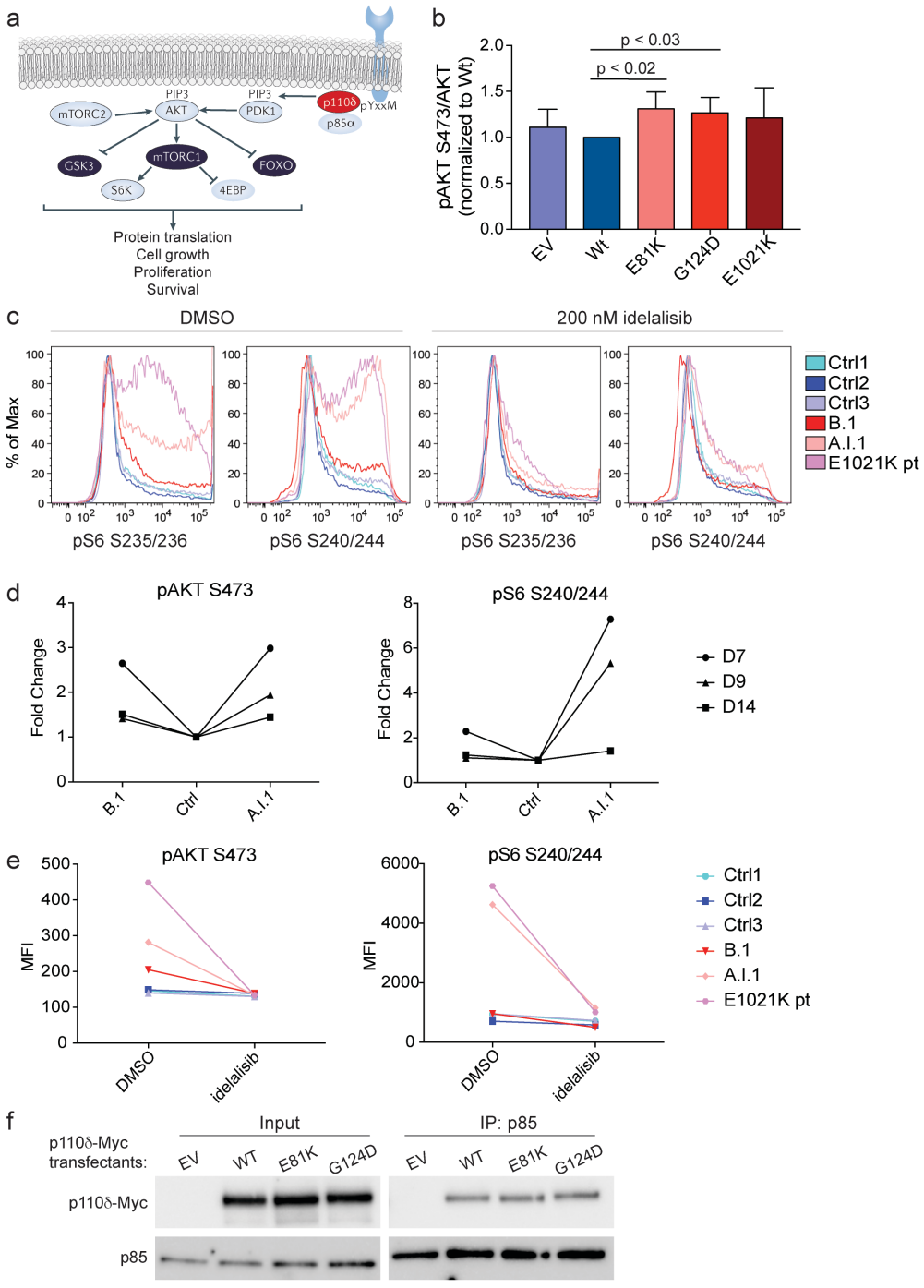
a
PIP3
PIP3
mTORC2
AKT
PDK1
p110δ
pYxxM
p85α
GSK3
mTORC1
FOXO
S6K
4EBP
Protein translation
Cell growth
Proliferation
Survival
b
p < 0.03
p < 0.02
pAKT S473/AKT (normalized to Wt)
2.0
1.5
1.0
0.5
0.0
EV
Wt
E81K
G124D
E1021K
c
DMSO
200 nM idelalisib
% of Max
pS6 S235/236
pS6 S240/244
pS6 S235/236
pS6 S240/244
Ctrl1
Ctrl2
Ctrl3
B.1
A.I.1
E1021K pt
d
pAKT S473
pS6 S240/244
Fold Change
B.1
Ctrl
A.I.1
D7
D9
D14
e
pAKT S473
pS6 S240/244
MFI
DMSO
idelalisib
Ctrl1
Ctrl2
Ctrl3
B.1
A.I.1
E1021K pt
f
Input
IP: p85
p110δ-Myc transfectants:
EV
WT
E81K
G124D
p110δ-Myc
p85

Figure E5